CHLORIDE CHANNELS IN THE EEL INTESTINE

A. BICHO, H. GIL FERREIRA AND K. GIL FERREIRA*

Departamento de Química, Centro de Química fina e Biotecnologia, Faculdade de Ciências e Tecnologia da Universidade Nova de Lisboa, 2825 Monte da Caparica, Portugal

*Present address and author for correspondence: Aldeamento das Encostas lote 20, Sassoeiros, 2775 Carcavelos, Portugal
(e-mail: karin.ferreira@dq.fct.unl.pt)

Summary

Patches of freshly isolated epithelial cells from eel *Anguilla anguilla* intestine bathed by the same solution on both sides in the cell-attached configuration had conductances of 57.0 ± 1.8 pS (for positive voltages) and 13.3 ± 0.7 pS (for negative voltages) (means ± S.E.M., $N=25$). Electrical activity was spontaneous in the cell-attached configuration, but was frequently lost after excision. In inside-out patches, channel activity was restored by strong hyperpolarization (-150 mV for 5 s) or depolarization ($+150$ mV for 5 s). Channel activity was inhibited by the Cl$^-$ transport blocker DIDS (1 mmol l^{-1}).

The membrane potential measured using the nystatin slow whole-cell technique in primary cultured eel intestine epithelial cells was -35.4 ± 1.0 mV ($N=14$), similar to the expected equilibrium potential for Cl$^-$ (-38.2 mV). Removal of Cl$^-$ from the bath or application of DIDS caused 16 mV and 6–7 mV depolarizing shifts in reversal potential, respectively. In one experiment, DIDS also induced a reduction in cell conductance from 0. 011 ± 0.014 to 0.002 ± 0.005 nS. The addition of 0.5 mmol l^{-1} 8-(4-chlorophenylthio)-adenosine 3′,5′-cyclic monophosphate (a membrane-permeable analogue of cyclic AMP) to the bath caused an increase in conductance without affecting the reversal potential.

Key words: Cl$^-$ channel, cyclic AMP, eel, intestine, *Anguilla anguilla*.

Introduction

The epithelium of the eel intestine is a single folded layer of columnar cells (Yamagishi et al., 1969; Ando and Kobayashi, 1978). In saltwater-adapted eels, it performs vigorous transepithelial coupled transport of NaCl and water from the mucosal to the serosal side (Ando, 1975, 1980, 1981, 1983, 1985). The use of transport inhibitors has indicated the presence of a 2Cl$^-$/Na$^+$/K$^+$ cotransporter in the apical barrier and a Na$^+$ pump together with a Na$^+$/Cl$^-$/HCO$_3^-$ antiporter and a K$^+$/Cl$^-$ symporter in the basolateral barrier (Marvão et al., 1994). Trischitta et al. (1992, 1996) were able to demonstrate an increase in transepithelial Cl$^-$ fluxes induced by cyclic AMP, presumably through the activation of Cl$^-$ channels.

The present study attempts to identify Cl$^-$ channels in the epithelial cells of eel intestine and investigates their contribution to the membrane potential and cell conductance.

Materials and methods
Cell isolation

Eels (*Anguilla anguilla* L.) freshly collected from the mouth of the river Tagus, Lisbon, Portugal, were kept at 4 °C in half-strength artificial sea water (230 mmol l^{-1} NaCl, 14 mmol l^{-1} MgSO$_4$). Animals were killed by decapitation and the medulla was destroyed. The posterior intestine was removed, opened and rinsed with NaCl solution (see below) containing 3 mmol l^{-1} dithiothreithol (DTT), a mucolytic agent. Epithelial cells were scraped off using a razor blade. They were then dissociated and cleaned enzymatically as follows: to 1 mg ml^{-1} collagenase and 1 mg ml^{-1} hyaluronidase in NaCl solution was added 1 mg ml^{-1} bovine serum albumin (BSA) and 3 mmol l^{-1} DTT. Cells were incubated in this medium at room temperature (22 °C) for between 45 and 60 min with gentle shaking. The cells were then washed twice by centrifugation (30 g, 2 min), resuspended in NaCl solution containing 1 mg ml^{-1} BSA and left on ice for 1–2 h.

Cell culture

Our procedures were based on those of Evans et al. (1994) and Booth et al. (1995) with slight modifications. The posterior intestine was washed several times in sterile NaCl solution containing 3 mmol l^{-1} DTT. Cells were scraped from the intestine and cleaned enzymatically by incubation in Dulbecco's minimum essential medium/nutrient Harris mixture F12 (1:1) (DMEM-F12) to which was added water (15 % v/v), 10 mmol l^{-1} Hepes, 2 mmol l^{-1} glutamine, 10 000 i.u. l^{-1} penicillin, 0.1 mg ml^{-1} streptomycin, 0.05 mg ml^{-1} gentamycin and heat-inactivated foetal bovine serum (10 % v/v). The cells were then centrifuged (30 g, 2 min). The pellet was resuspended in an enriched DMEM-F12

culture medium containing $0.01\,\mathrm{mg\,ml^{-1}}$ insulin, $1\,\mathrm{\mu g\,ml^{-1}}$ fibronectin and $0.02\,\mathrm{mg\,ml^{-1}}$ transferrin. Finally, the cells were plated onto collagen-coated Petri dishes and kept at $20\,^{\circ}\mathrm{C}$. After 48 h, cell clusters were adherent and starting to form a monolayer (Fig. 1A). After a further 48 h, the medium was removed, with most of the dead cells and debris, and replaced with fresh medium. Cells had migrated from the initial cell groups and combined to form larger monolayers (Fig. 1B); these started to detach 1 week after seeding. Cells were studied 3–6 days after seeding.

Patch-clamp studies

Single-channel experiments

We applied the cell-attached and the inside-out configurations of the patch-clamp technique (Hamill et al., 1981) to isolated cells, which were then plated onto glass coverslips attached to the bottom of Petri dishes pretreated with poly-L-lysine (0.1 % v/v).

Borosilicate filamented glass pipettes (o.d. 1.5 mm; i.d. 0.86 mm) were pulled in two steps in a vertical puller, fire-polished and coated with Sylgard. The best seals were obtained with $15\,\mathrm{M\Omega}$ pipettes when filled with NaCl solution. The reference electrode was a Ag/AgCl wire embedded in a $1\,\mathrm{mol\,l^{-1}}$ KCl/agar bridge.

Solutions

The NaCl solution contained (in $\mathrm{mmol\,l^{-1}}$) 120 NaCl, 5 KCl, 3 $CaCl_2$, 1 $MgCl_2$, 5 Hepes, 5 sodium pyruvate, 5 glucose (pH 7.4, $265\,\mathrm{mosmol\,kg^{-1}}$). The K^+ solution contained (in $\mathrm{mmol\,l^{-1}}$) 10 NaCl, 115 KCl, 3 $CaCl_2$, 1 $MgCl_2$, 5 Hepes, 1 EGTA, 5 sodium pyruvate, 5 glucose (pH 7.2, $255\,\mathrm{mosmol\,kg^{-1}}$). We also added 3–6 $\mathrm{mmol\,l^{-1}}$ $BaCl_2$ to the pipette solution to block K^+ channels. All the pipette solutions were filtered through a Millipore filter (MILLEX-GS, SLGS 025 BS, pore diamter $0.22\,\mathrm{\mu m}$). A stock solution of the Cl^- channel blocker 4,4′-diisothiocyanatostilbene-2,2′-disulphonic acid (DIDS) ($1\,\mathrm{mmol\,l^{-1}}$) in dimethylsulphoxide (DMSO) was kept in the dark. Fresh solutions of the desired concentration were prepared every 2 h on the day of each

experiment. The concentration of DMSO in the final solutions was 0.1 %. Bath solutions were changed gravimetrically or fed by syringe injection at a flow rate of 5–10 $\mathrm{ml\,min^{-1}}$. The time for 90 % turnover of the solution in the Petri dish was 37 s.

Whole-cell experiments

Conventional whole-cell techniques proved difficult to apply to freshly isolated cells. Even gentle negative pressure caused cells to be sucked into the pipette. We used instead the slow whole-cell (SWC) configuration of the patch-clamp technique (Horn and Marty, 1988; Oleson et al., 1993) applied to cells from primary cultures of epithelial cells of eel intestine. The adherence of these cells to the dishes facilitated seal formation, but the rate of success remained poor. The volume of nystatin-free solution at the tip of the pipette varied between experiments and, consequently, the rate of diffusion of nystatin into the membrane patch also varied. Cell-attached patches became perforated 3–20 min after seal formation.

Results obtained from freshly isolated cells and from cultured cells were very similar and were pooled. The cultured cells were pretreated with DTT ($3\,\mathrm{mmol\,l^{-1}}$) in NaCl solution. Electrodes ($4\,\mathrm{M\Omega}$), prepared as described above but from unfilamented borosilicate glass, were filled with a K^+-rich solution containing (in $\mathrm{mmol\,l^{-1}}$) 20 NaCl, 10 KCl, 1 $CaCl_2$, 3 $MgCl_2$, 5 Hepes, 1 EGTA, 100 potassium gluconate, 1 NaATP (pH 7.2, $230\,\mathrm{mosmol\,kg^{-1}}$). To improve seal formation, a slightly hypotonic solution (80 % of cell osmolality) was used. Before each set of experiments, ATP (to $5\,\mathrm{mmol\,l^{-1}}$) was added to the pipette solution, which was then filtered through a Millipore filter (MILLEX-GS, SLGS 025 BS, pore diameter $0.22\,\mathrm{\mu m}$). Freshly prepared nystatin (100–300 $\mathrm{mg\,ml^{-1}}$ in DMSO) was dissolved in 10 ml of the previously prepared pipette solution and sonicated. The tips of the pipettes were filled by dipping them in the nystatin-free solution. The pipettes were then back-filled with the nystatin-containing solution. The nystatin solution was kept on ice and in the dark for up to 2 h. During the experiments, the microscope light was

Fig. 1. Phase-contrast photographs of a primary culture of eel intestine cells. (A) Photograph taken 48 h after seeding showing several small adherent cell clusters with migrating cells. Non-adherent globular isolated cells can still be observed (arrows). (B) Photograph taken 96 h after seeding showing further cell migration and growth from the plated cell groups. The large cell monolayer is formed by the combination of several initial cell colonies. It is possible to identify cell debris from the original plated cells (arrows). Scale bars, $100\,\mathrm{\mu m}$.
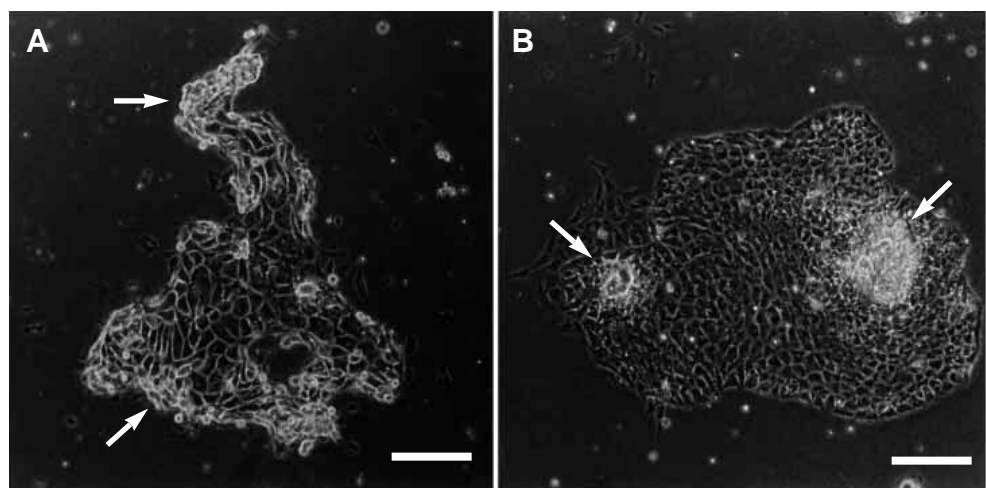
switched off whenever possible. The reference electrode was as described above.

Intracellular electrical potential and membrane currents were measured using the following solutions in the external bath: NaCl solution (see above); and nominally Cl$^-$-free solution (in mmol l^{-1}), 120 sodium gluconate, 5 potassium gluconate, 3 calcium gluconate, 1 magnesium acetate, 5 Hepes, 5 sodium pyruvate, 5 glucose (pH 7.4, 260 mosmol kg^{-1}). DIDS (0.4 mmol l^{-1}) and a permeable analogue cyclic AMP (sodium salt, 0.5 mmol l^{-1}) were dissolved in NaCl solution. Bath solution changes were performed as described above.

Data acquisition and analysis

Currents were recorded at room temperature (22 °C) using an Axopatch-1D patch-clamp amplifier (Axon Instruments). Commercial software from Axon Instruments was used for the voltage-clamp protocols, data acquisition and data analysis. All command voltages and membrane currents are analysed as if they had been measured at the intracellular side of the membrane. In both the whole-cell and inside-out configurations, the applied potentials correspond to the difference between the bath and pipette potentials. In cell-attached patches, the applied potential is superimposed on the spontaneous cell membrane potential, which is assumed to be −33 mV under the experimental conditions (Marvão et al., 1994). Junction potentials were zeroed before seal formation, and for whole-cell experiments we also corrected the potential values for the liquid junction potentials arising from the use of different solutions in the pipette and bath or from changes in bath solution.

Analysis of single-channel recordings was performed if only one current level was present. Reversal potentials and conductance values were obtained from current–voltage (*I/V*) plots. Reversal potentials in the cell-attached configuration were estimated using the intracellular Cl$^-$, K$^+$ and Na$^+$ concentrations reported by Marvão et al. (1994). When rectification was present, the asymptotic forward and backward conductances were estimated using least-mean-square linear fitting. Reversal potentials were estimated by interpolation after fitting polynomial functions to the *I/V* curves. In slow whole-cell experiments, we considered that nystatin had diffused into the cell membrane and that the system entered the whole-cell configuration when cell membrane potential monitored in the current-clamp mode (*I*=0 A) reached a steady state (variation ≤0.5 % min^{-1}). *I/V* curves were obtained in the voltage-clamp mode.

Results are presented as original recordings or *I/V* plots. When results from more than two cells are presented, mean values ± standard errors of the mean (S.E.M.) are plotted. The number of experiments is given in parentheses.

The values of the concentrations used are not corrected for activity. When comparisons with published values that had been corrected for activity are made, these were converted to conventional concentrations using activities given by Robinson and Stokes (1959) and assuming an ionic strength of 150 mmol l^{-1} KCl solution.

Chemicals

The culture medium and all other chemicals used in cell cultures were purchased from Gibco (Paisley, Renfrewshire, Scotland, UK). Collagen and Sylgard were obtained from Biochrom (Berlin, Germany) and Dow Corning Corp. (Midland, MI 48640, USA), respectively. All other substances were purchased from Sigma (St Louis, MI, USA).

Results

Single-channel results

Fig. 2A shows single-channel Cl$^-$ currents recorded in the cell-attached configuration at different membrane potentials, with NaCl solution in both the pipette and the bath. A mean *I/V* curve from several patches (*N*=25) recorded under the same conditions is shown in Fig. 2B. The reversal potential of −36±2 mV (*N*=25) is closer to the estimated equilibrium potential for Cl$^-$ (−23 mV) under these conditions than to the estimated equilibrium potentials for K$^+$ (−77 mV) or Na$^+$ (+34 mV). The slope conductances were 57.0±1.8 pS for the outward current and 13.3±0.7 pS for the inward current. In inside-out patches (*N*=3) (Fig. 2C), the reversal potential was again close to the predicted Cl$^-$ equilibrium potential. With NaCl solution in the pipette and KCl solution in the bath, giving almost the same Cl$^-$ concentration on both sides of the membrane patch, the outward slope conductance was 61.5±2.2 pS and the inward slope conductance was 32.2±0 pS, the ratio of outward to inward conductance being 1.91. The reversal potential in these experiments was −3.8 mV.

Most of our results are from the cell-attached configuration because patch excision frequently caused the disappearance of channel activity. Channel activity could be restored by the application of a strong hyperpolarizing (−150 mV for 5 s) or depolarizing (+150 mV for 5 s) voltage (Fig. 3A,B), but in most of our experiments we lost the seal. Fig. 3 shows a sequence of current recordings after the disappearance of channel activity when the membrane patch was excised (Fig. 3A). Activity reappeared when the patch was depolarized to 150 mV for 5 s (Fig. 3B) and was blocked by the addition of DIDS (1 mmol l^{-1}) to the bath (Fig. 3C). Similar results were obtained in five other experiments.

Whole-cell results

Fig. 4 presents cell membrane potentials (*V*$_m$) at zero patch current during a sequence of bath solution changes. The stable *V*$_m$ values obtained with NaCl solution in the bath averaged −35.4±1.0 mV (*N*=14). These values are comparable with those (−33.4±1.0 mV, *N*=59) found by Marvão et al. (1994) using intracellular microelectrodes. Our major finding is that a rapid change in bath Cl$^-$ concentration from 130 mmol l^{-1} to a nominal 0 mmol l^{-1} produced a depolarization of 16±2 mV (*N*=6). This is a strong indication that the membrane of these cells is mainly Cl$^-$-selective. This effect was completely reversed by restoring the initial Cl$^-$ concentration. Further evidence for Cl$^-$ selectivity comes
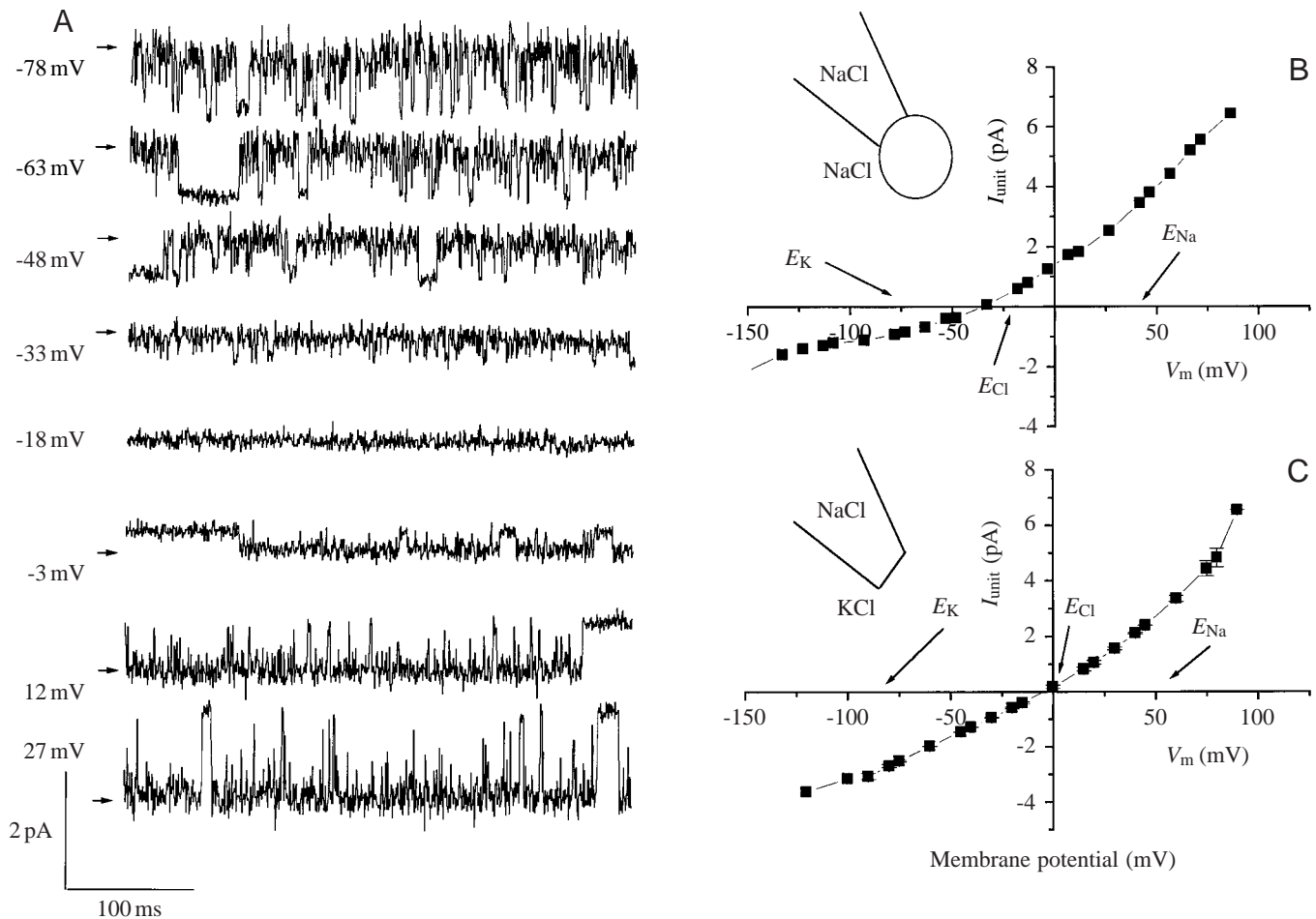
Fig. 2. Single-channel Cl⁻ currents in isolated epithelial cells of eel intestine. (A) Recordings of currents in the cell-attached configuration at different membrane potentials (V_m) with NaCl solution in the pipette and bath. Note the long periods during which channels were open interrupted by brief closing events. Arrows indicate the channel-open state. (B) Mean current–voltage (*I/V*) curve recorded from patches (*N*=25) under the same conditions as in A. Estimated equilibrium potentials for Cl⁻ (E_{Cl}) (also *x* intercept in figure), K⁺ (E_K) and Na⁺ (E_{Na}) are indicated by arrows. Values are means ± S.E.M. (C) Mean *I/V* curve recorded using the inside-out configuration with the pipette filled with NaCl solution and the bath containing KCl solution (*N*=3). Values are means ± S.E.M. Estimated equilibrium potentials for Cl⁻, K⁺ and Na⁺ are indicated by arrows. The measured reversal potential is close to that expected for Cl⁻. The insets in B and C represent the cell-attached and inside-out configurations, respectively, and show the solutions used. I_{unit}, unit current.

from the observation that, in two experiments, the addition of 0.4 mmol l⁻¹ DIDS to the bath solution produced a 6–7 mV depolarization of V_m. Cell membrane potential recordings showed a small hyperpolarization of only approximately 3 mV after the addition of 0.5 mmol l⁻¹ cyclic AMP to the bath solution. At the concentrations used, these effects of cyclic AMP and DIDS on V_m were completely reversible when the bathing solution was replaced with 130 mmol l⁻¹ NaCl solution.

In a few experiments, it was possible to measure cell currents in the voltage-clamp mode, and the results are shown in Fig. 5. The voltage range applied to the cells was very narrow (−60 to +60 mV) owing to limitations in seal stability. In one experiment, the traditional whole-cell configuration was obtained spontaneously and the conductance was similar to that induced by nystatin in the other experiments. Fig. 5A

shows a typical *I/V* plot in control conditions with NaCl as the bath solution; the reversal potential (V_r) of −37.6 mV is near the calculated Cl⁻ equilibrium potential of −38.2 mV. We found similar *I/V* curves in 12 different cells. The possible contribution of Cl⁻ to the cell conductance was studied in five different cells by removing Cl⁻ from the bathing medium; a typical result is shown in Fig. 5B. When bath Cl⁻ concentration was lowered to a nominal 0 mmol l⁻¹, the cell conductance decreased and the reversal potential shifted from −40 to −21.9 mV. This effect was reversible (data not shown). The effect of cyclic AMP was also studied (Fig. 5C). Addition of 0.5 mmol l⁻¹ cyclic AMP to the bath NaCl solution induced an increase in cell conductance without shifting the reversal potential (*N*=2). In one experiment, we studied the inhibitory effect of DIDS on these cell currents (Fig. 5D). At a bath concentration of
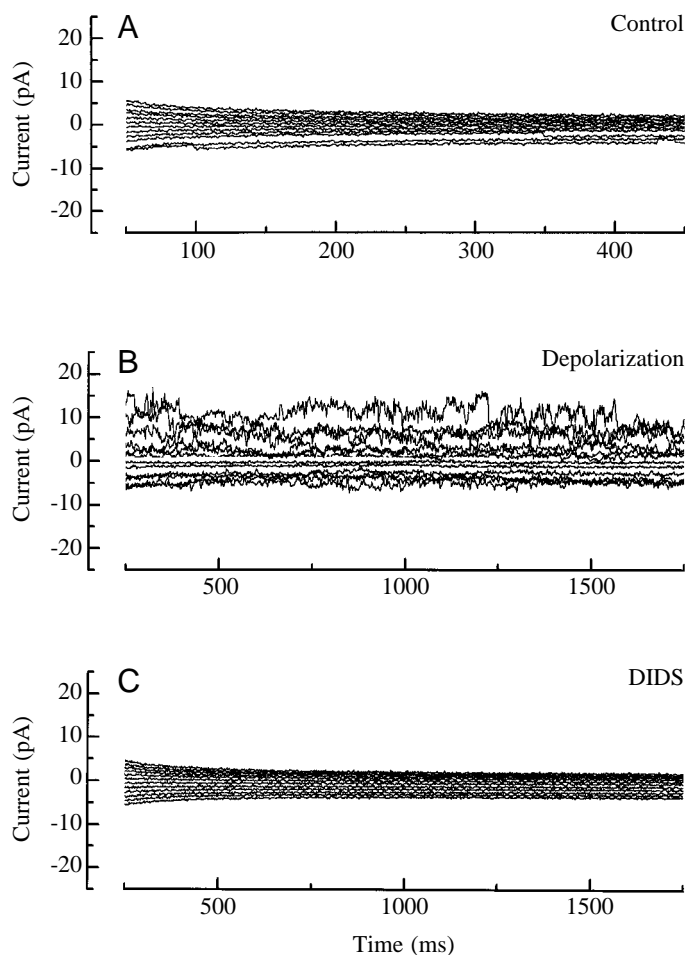
Fig. 3. Single-channel currents recorded from an inside-out patch from an isolated epithelial cell of the eel intestine at different membrane potentials (−100 to +120 mV in steps of 20 mV). NaCl solution was in the pipette and KCl solution in the bath. (A) Recording from an inside-out patch immediately after excision. Almost no channel activity is present. (B) Recording after depolarization to +150 mV for 5 s. (C) Recording after the addition of 1 mmol l^{-1} DIDS to the bath. Note the complete inhibitory effect of DIDS on channel activity.

0.4 mmol l^{-1}, the conductance decreased slowly from 0.011±0.014 nS to 0.002±0.005 nS over 20 min. This effect was not completely reversible (results not shown).

Discussion

By using the cell-attached and the inside-out configurations of the patch-clamp technique, it was possible to identify and characterise one type of Cl^{-} channel in eel intestine epithelial cells. In cell-attached experiments, we found that Cl^{-} currents reversed at −36 mV instead of at the expected value of −23 mV estimated from the intracellular Cl^{-} concentration (54 mmol l^{-1}) determined by Marvão et al. (1994). The intracellular Cl^{-} concentration corresponding to the experimental reversal potential was 33 mmol l^{-1}, similar to
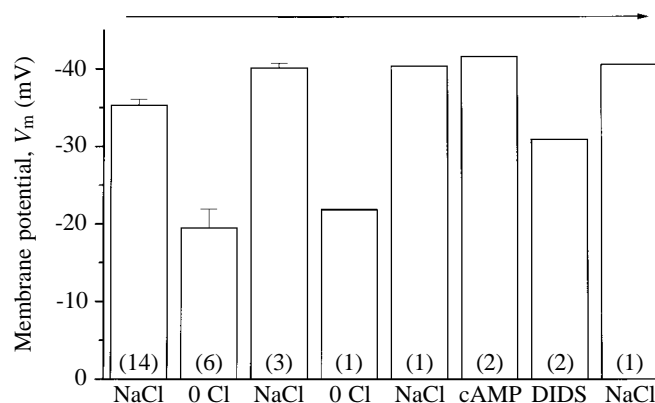

Fig. 4. Zero-current recordings (*N*=14) of cell membrane potential (*V*$_m$) in nystatin–perforated patches (slow whole-cell method). Values are means, with S.E.M. where *N*⩾2. The number of measurements is given in parentheses. Cyclic AMP (0.5 mmol l^{-1}) and DIDS (0.4 mmol l^{-1}) were dissolved in NaCl solution. The arrow indicates the time sequence of changes in the bathing solution. Note that the depolarization caused by 0.4 mmol l^{-1} DIDS is not as great as the depolarization caused by the removal of Cl^{-} from the bath solution.

values measured directly using double-barrelled Cl^{-} microelectrodes: 27.4 mmol l^{-1} in isolated frog (*Rana temporaria*) epidermis (Giraldez and Ferreira, 1984), 22.5 mmol l^{-1} in toad (*Bufo bufo*) skin epithelium (Willumsen and Hviid Larsen, 1986), 37.7 and 32.8 mmol l^{-1} in frog (*Rana ridibunda pallas*) skin epithelium (Fernandes et al., 1989) and 30.8 mmol l^{-1} in isolated rabbit caecum (Ferreira et al., 1992). This discrepancy might be due to an overestimation of intracellular Cl^{-} content by Marvão et al. (1994), but one should keep in mind that there is a vigorous 'active' uptake of Cl^{-} across the apical barrier in fish intestine. Alternatively, the Cl^{-} gradient might be dissipated in the isolated cells or other ion channels might contribute to the cell reversal potential.

In the inside-out configuration, the reversal potential of the current pulses was near zero when the electrochemical potential difference for Cl^{-} was also zero, regardless of whether non-zero electrochemical gradients for Na^{+} and K^{+} were applied simultaneously. This indicates that either highly selective Cl^{-} channels or non-specific cation channels are present. The first explanation is supported by the observation that channel activity was completely blocked by 1 mmol l^{-1} DIDS.

The current–voltage relationships obtained from patches in the cell-attached and inside-out configurations were non-linear over the voltage range studied and showed outward rectification. Our results are similar to those for intermediate outward-rectifying Cl^{-} channels (IORCs) (Hayslett et al., 1987; Gray et al., 1989; Frizzell and Halm, 1990; Poncet et al., 1994).

Channel activity was spontaneous in the cell-attached configuration, but frequently disappeared after excision of
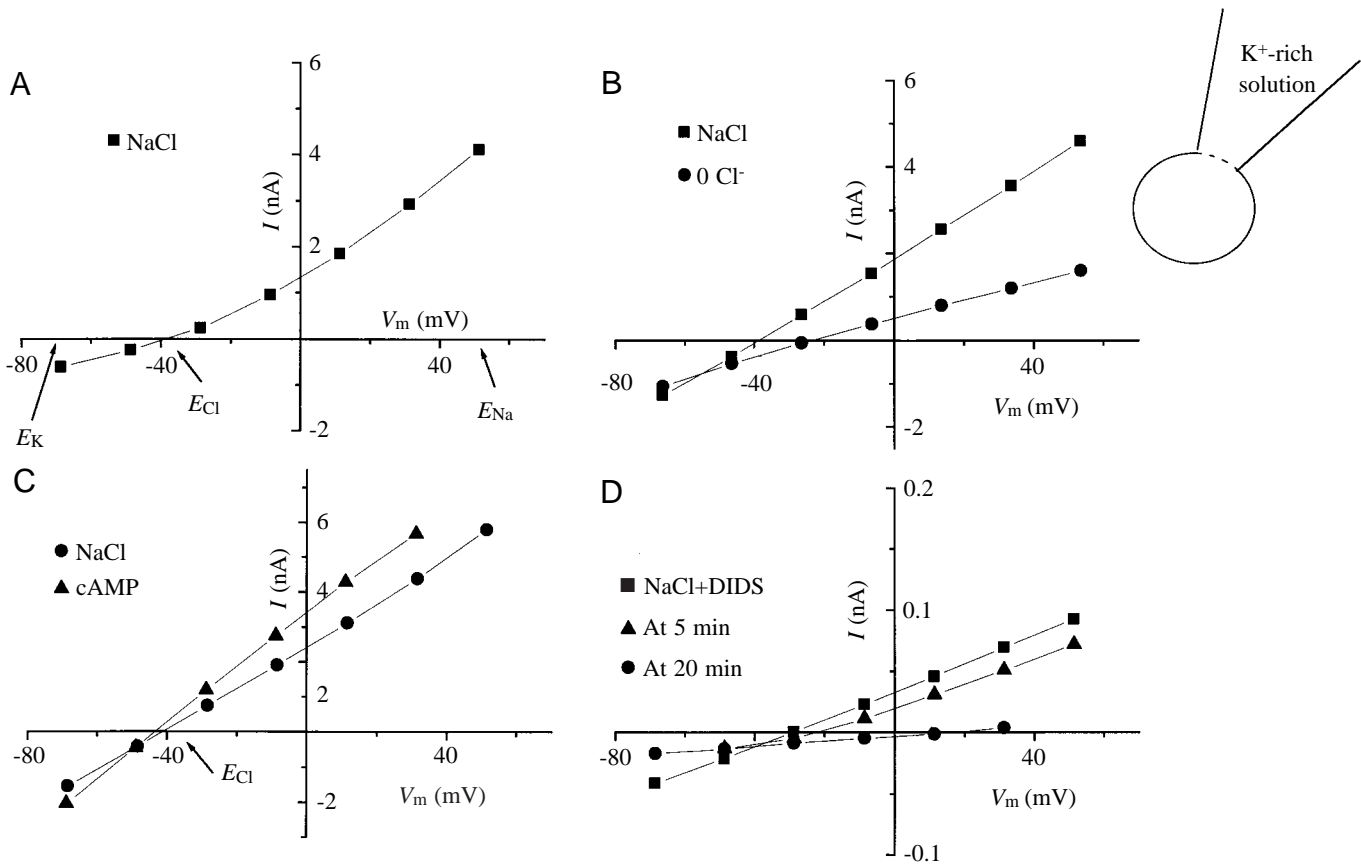
Fig. 5. Current–voltage (I/V) curves in perforated patches (nystatin slow whole-cell method) from primary cultured cells of eel intestine. (A) Pipette filled with K$^+$-rich solution and NaCl solution in the bath. Estimated equilibrium potentials for Cl$^-$ (E_{Cl}), Na$^+$ (E_{Na}) and K$^+$ (E_K) are indicated by arrows. (B) Effect of replacement of 120 mmol l^{-1} NaCl solution with Cl$^-$-free solution in the bath. (C) Effect of addition of 0.5 mmol l^{-1} cyclic AMP to the NaCl bath solution. The x intercept is very near the estimated E_{Cl} and is not changed by addition of cyclic AMP. (D) Effect of addition of 0.4 mmol l^{-1} DIDS to the NaCl bath solution. The first curve (■) was measured immediately. Complete inhibition occurs only after 20 min. The inset represents the nystatin slow whole-cell configuration with K$^+$-rich solution in the pipette. I, current; V_m, membrane potential.

the patch. In cells such as goby (*Gillichthys mirabilis*) intestinal cells (Loretz and Fourtner, 1988), cultured human airway cells (Kunzelmann et al., 1989), HT$_{29}$ cells derived from human colon carcinoma (Kunzelmann et al., 1991; Krick et al., 1991), human placenta trophoblasts (Kunzelmann et al., 1991) and pig kidney cortex cells (Krick et al., 1991), some IORCs are regulated by cytosolic factors. This suggests the presence of cytosolic inhibitors. In epithelial cells from eel intestine, we found that spontaneous activity in the cell-attached configuration disappeared after excision. We suggest that the channels in this case may be regulated positively by some intracellular factor that is lost or diluted after excision. Additionally, our experiments showed that these channels are voltage-regulated. After patch excision, we could frequently restore channel activity by briefly (5 s) depolarising (+150 mV) or hyperpolarising (−150 mV) transmembrane voltages. There are examples in the literature of activation of epithelial Cl$^-$ channels in excised membrane patches by strong sustained depolarisation (Gray et al., 1989; Solc and Wine, 1991;

Anderson et al., 1992; Poncet et al., 1994). These channels differ from those described here since they are mostly silent in cell-attached patches, although activation can be induced following excision.

We further investigated the contribution of possible ionic conductances to eel intestine epithelial cell membrane potential using the nystatin slow whole-cell (SWC) configuration of the patch-clamp technique. In these experiments, the K$^+$ channel inhibitor Ba^{2+} was not used. Our results revealed that the membrane conductance of epithelial cells of the eel intestine is mainly Cl$^-$-selective. In these experiments, we clamped the current at 0 A and followed changes in the membrane potential that occurred as a result of ion substitutions. We found (a) that the membrane potential measured in control conditions (−35.4 mV) was similar to the estimated equilibrium potential for Cl$^-$ (−38.2 mV), (b) that a strong depolarisation was caused by removal of Cl$^-$ from the bath solution, and (c) that a depolarization was observed in the presence of the Cl$^-$ channel blocker DIDS.

The current–voltage curves indicate that the cell

conductance is mainly due to Cl⁻ channels since (a) when a sufficient range of voltages could be applied (without losing the seals), the whole-cell I/V curves were similar to those found in single-channel experiments, with outward rectification and a reversal potential of -35.4 mV ($I=0$ A), similar to the estimated Cl⁻ equilibrium potential, (b) there was a decrease in conductance when the Cl⁻-containing bathing medium was replaced with a nominally Cl⁻-free solution, and (c) the Cl⁻ channel blocker DIDS blocked the cell conductance.

In one experiment in the whole-cell configuration, the application of 0.4 mmol l⁻¹ DIDS caused a marked reduction in cell conductance and a shift in the reversal potential towards the Na⁺ equilibrium potential (50.2 mV). However, in single-channel experiments, we did not detect Na⁺ channels. We found that the same concentration of DIDS caused a 6–7 mV depolarising shift in reversal potential in the experiments in which we followed the cell membrane potential. This difference is probably due to a shorter period of inhibition since 0.4 mmol l⁻¹ DIDS applied for 20 min caused complete current inhibition.

Perforated patch experiments showed that 0.5 mmol l⁻¹ cyclic AMP in the bath solution caused an increase in cell conductance without a concurrent shift in the reversal potential. This implicates activation of channels already present, probably Cl⁻-selective channels. It has been suggested that cyclic AMP or its agonists activate Cl⁻ channels in secretory epithelia in human colon (HT₂₉) cells (Hayslett et al., 1987) and in cultured human airway epithelial cells (Schwiebert et al., 1994; for a review, see Anderson et al., 1992). In eel intestine, Trischitta et al. (1996) demonstrated that cyclic AMP activates transcellular Cl⁻ conductance mechanisms.

Whether Cl⁻ channels exist only on the apical membrane or also in the basolateral membrane remains to be investigated. On the basis of the large Cl⁻ fluxes found in either the serosal or the mucosal direction (with a net flux towards the serosal side), Marvão et al. (1994) predicted the existence of Cl⁻ channels on both the apical and basolateral barriers. Our single-channel current experiments were performed on freshly isolated epithelial cells from eel intestine or on cultured cells. Therefore, for these preparations, we could not define the precise location of the channels. We observed single-current events in almost all experiments with isolated cells, an indication that these channels may occur on both cell membranes.

References

Anderson, M. P., Sheppard, D. N., Berger, H. A. and Welsh, M. J. (1992). Chloride channels in the apical membrane of normal and cystic fibrosis airway and intestinal epithelia. *Am. J. Physiol.* **263**, L1–L14.

Ando, M. (1975). Intestinal water transport and chloride pump in relation to sea-water adaptation of the eel, *Anguilla japonica. Comp. Biochem. Physiol.* **52**A, 229–233.

Ando, M. (1980). Chloride-dependent sodium and water transport in the seawater eel intestine. *J. Comp. Physiol.* **138**, 87–91.

Ando, M. (1981). Effects of ouabain on chloride movements across the seawater eel intestine. *J. Comp. Physiol.* **145**, 73–79.

Ando, M. (1983). Potassium-dependent chloride and water transport across the seawater eel intestine. *J. Membr. Biol.* **73**, 125–130.

Ando, M. (1985). Relationship between coupled Na⁺–K⁺–Cl⁻ transport and water absorption across the seawater eel intestine. *J. Comp. Physiol.* **155**, 311–317.

Ando, M. and Kobayashi, M. (1978). Effects of stripping of the outer layers of the eel intestine on salt and water transport. *Comp. Biochem. Physiol.* **61**A, 497–501.

Booth, C., Patel, S., Bennion, G. R. and Potten, C. S. (1995). The isolation and culture of adult mouse colonic epithelium. *Epith. Cell Biol.* **4**, 76–86.

Evans, G. S., Flint, N. and Potten, C. S. (1994). Primary cultures for studies of cell regulation and physiology in intestinal epithelium. *Annu. Rev. Physiol.* **56**, 399–417.

Fernandes, P. L., Ferreira, H. G. and Ferreira, K. T. G. (1989). The coupled movements of sodium and chloride across the basolateral membrane of frog skin epithelium. *J. Physiol., Lond.* **416**, 403–420.

Ferreira, K. T. G., Fernandes, P. L. and Ferreira, H. G. (1992). Ion transport across the epithelium of rabbit caecum. *Biochim. Biophys. Acta* **1175**, 27–36.

Frizzell, R. A. and Halm, D. R. (1990). Chloride channels in epithelial cells. In *Current Topics in Membranes and Transport*, vol. 37 (ed. F. Bronner, W. V. Driessche and S. I. Helman), pp. 247–282. New York: Academic Press.

Giraldez, F. and Ferreira, K. T. G. (1984). Intracellular chloride activity and membrane potential in stripped frog skin (*Rana temporaria*). *Biochim. Biophys. Acta* **769**, 625–628.

Gray, M. A., Harris, A., Coleman, L., Greenwell, J. R. and Argent, B. E. (1989). Two types of chloride channel on duct cells cultured from human fetal pancreas. *Am. J. Physiol.* **257**, C240–C251.

Hamill, O. P., Marty, A., Neher, E., Sakmann, B. and Sigworth, J. F. (1981). Improved patch-clamp techniques for high-resolution current recording from cells and cell-free membrane patches. *Pflügers Arch.* **391**, 85–100.

Hayslett, J. P., Gögelein, H., Kunzelmann, K. and Greger, R. (1987). Characteristics of apical chloride channels in human colon cells (HT₂₉). *Pflügers Arch.* **410**, 487–494.

Horn, R. and Marty, A. (1988). Muscarinic activation of ionic currents measured by a new whole-cell recording method. *J. Gen. Physiol.* **92**, 145–159.

Krick, W., Disser, J., Hazama, A., Burckhardt, G. and Frömter, E. (1991). Evidence for a cytosolic inhibitor of epithelial chloride channels. *Pflügers Arch.* **418**, 491–499.

Kunzelmann, K., Pavenstädt, H. and Greger, R. (1989). Properties and regulation of chloride channels in cystic fibrosis and normal airway cells. *Pflügers Arch.* **415**, 172–182.

Kunzelmann, K., Tilmann, M., Hansen, Ch. P. and Greger, R. (1991). Inhibition of epithelial chloride channels by cytosol. *Pflügers Arch.* **418**, 479–490.

Loretz, C. A. and Fourtner, C. R. (1988). Funtional characterization of a voltage-gated anion channel from teleost fish intestinal epithelium. *J. Exp. Biol.* **136**, 383–403.

Marvão, P., Emílio, M. G., Ferreira, K. G., Fernandes, P. L. and Ferreira, H. G. (1994). Ion transport in the intestine of *Anguilla anguilla*: gradients and translocators. *J. Exp. Biol.* **193**, 97–117.

Oleson, D. R., DeFelice, L. J. and Donahoe, R. M. (1993). A

comparison of K$^+$ channel characteristics in human T cell: Perforated-patch *versus* whole-cell recording techniques. *J. Membr. Biol.* **132**, 229–241.

Poncet, V., Tauc, M., Bidet, M. and Poujeol, P. (1994). Chloride channels in the apical membrane of primary cultures of rabbit distal bright convoluted tubule. *Am. J. Physiol.* **266**, F543–F553.

Robinson, R. A. and Stokes, R. H. (1959). The measurement of chemical potentials. In *Electrolyte Solutions*. London: Butterworths. pp. 174–222.

Schwiebert, E. M., Flotte, T., Cutting, G. R. and Guggino, W. B. (1994). Both CFTR and outwardly rectifying chloride channels contribute to cyclic AMP-stimulated whole cell chloride currents. *Am. J. Physiol.* **266**, C1464–C1477.

Solc, C K. and Wine, J. J. (1991). Swelling-induced and depolarization-induced Cl$^-$ channels in normal and cystic fibrosis epithelial cells. *Am. J. Physiol.* **261**, C658-C674.

Trischitta, F., Denaro, M. D., Faggio, C., Mandolfino, M. and Schettino, T. (1996). Different effects of cGMP and cAMP in the intestine of the European eel, *Anguilla anguilla*. *J. Comp. Physiol.* **166**, 30–36.

Trischitta, F., Denaro, M. G., Faggio, C. and Schettino, T. (1992). An attempt to determine the mechanisms of chloride exit across the basolateral membrane of eel intestine: use of different chloride transport pathway inhibitors. *J. Exp. Zool.* **264**, 11–18.

Willumsen, N. J. and Hviid Larsen, E. (1986). Membrane potentials and intracellular Cl$^-$ activity of toad skin epithelium in relation to activation and deactivation of the transepithelial Cl$^-$ conductance. *J. Membr. Biol.* **94**, 173–190.

Yamagishi, I., Nagumo, N., Oshiro, S., Suzuki, T., Oya, T. and Muraki, T. (1969). Electron microscopic observation on the absorptive epithelium of the eel intestine. *J. Med. Soc. (Toho)* **16**, 101–108.